

Spin gap in $\text{CeFe}_4\text{Sb}_{12}$ studied by heat capacity and inelastic neutron scattering

R. Viennois,^{1,2,3} L. Girard,² L. C. Chapon,⁴ D. T. Adroja,^{4,*} R. I. Bewley,⁴ D. Ravot,² Peter. S. Riseborough,⁵ and S. Paschen^{3,†}

¹DPMC, Université de Genève, 24 Quai Ernest Ansermet, CH-1211 Genève 4, Switzerland

²LPMC, Université Montpellier II, Place Eugène Bataillon, F-34095 Montpellier, France

³Max-Planck-Institut für Chemische fester Stoffe, Nöthnitzer Strasse 40, D-01185 Dresden, Germany

⁴ISIS Facility, Rutherford Appleton Laboratory, Chilton Didcot, Oxfordshire OX11 0QX, United Kingdom

⁵Department of Physics, Temple University, Barton Hall, 1900 North 13th Street, Philadelphia, Pennsylvania 19122, USA

(Received 17 May 2007; revised manuscript received 14 September 2007)

The magnetic properties of the skutterudite compound $\text{CeFe}_4\text{Sb}_{12}$ have been investigated by heat capacity and inelastic neutron scattering measurements. Heat capacity measurements reveal a broad peak centered at 125 K, whose magnitude is much larger than that expected from a Schottky anomaly due to a cubic crystal electric field. At 5 K, inelastic neutron scattering experiments clearly show the existence of a broad magnetic peak at 40(3) meV. The absence of quasielastic scattering at this temperature, together with the almost total account of the magnetic signal in the inelastic peak, shows that the excitation has a different origin than a splitting of the electronic levels due to crystal field energy. Instead, we propose a model in which the signal originates from inelastic excitations across two hybridization bands near the Fermi energy, usually referred to as a spin gap. A simple phenomenological two-level model can account for the peak in the specific heat, with a spin-gap energy of 36(2) meV, which is in very good agreement with the inelastic scattering data. Further, at 300 K, the inelastic response becomes purely quasielastic, which is in agreement with the theoretical calculations. Interestingly, the spin-gap energy in $\text{CeFe}_4\text{Sb}_{12}$ exhibits a universal scaling behavior with the Kondo temperature T_K . The relation between the spin-gap energy and the associated anomalies in the heat capacity or thermal expansion is discussed for a series of Ce- and Yb-based compounds.

DOI: XXXX

PACS number(s): 75.30.Mb, 71.27.+a, 75.20.Hr, 72.15.Qm

I. INTRODUCTION

For more than a decade, the filled skutterudite compounds with the general formula RM_4X_{12} (R =rare or alkaline earth, actinide or alkaline metal, M =transition metal, and X =P, As, or Sb) have attracted considerable attention primarily because of their enhanced thermoelectric properties¹ and potential applications in future solid state devices. These compounds have generated a great deal of interest in the physics community due to their diverse and complex physical properties, as seen from the existence of many exotic ground states, notably, unconventional superconductivity,² quadrupolar ordering,³ metal-insulator transition,⁴ non-Fermi liquid behavior⁵⁻⁷ and hybridization gap (or pseudogap) semimetal.⁷⁻¹⁰ Among these properties, the hybridization gap is one of the most investigated phenomena in many Ce-based compounds, such as in $\text{CeRu}_4\text{Sb}_{12}$, $\text{CeFe}_4\text{Sb}_{12}$, and $\text{CeOs}_4\text{Sb}_{12}$.⁷⁻¹⁰ A hybridization gap is a gap in the electronic density of states (DOS) near the Fermi energy (E_F), which opens due to the presence of strong hybridization between localized $4f$ electrons and conduction electrons. Interestingly, despite the existence of a hybridization pseudogap, these compounds exhibit a non-Fermi liquidlike (NFL) behavior at low temperatures.^{6,7} We have previously shown that all the aforementioned Ce compounds have very similar physical properties,^{7,10} although isolating the contribution of the Ce ion in $\text{CeFe}_4\text{Sb}_{12}$ was found to be difficult due to the large contribution of Fe to the physical properties at low temperatures, especially to the magnetic properties.⁷

Recently, both charge and spin pseudogaps have been detected in $\text{CeRu}_4\text{Sb}_{12}$ by optical spectroscopy and inelastic

neutron scattering experiments, respectively, and have the same order of magnitude while having slightly different values.^{8,9} Interestingly, the ratio between these values of energy agrees well with existing theories.¹¹ In optical studies, within a first order dipole approximation, one observes a direct gap at wave vector $Q=0$, while in inelastic neutron scattering studies, one normally observes an indirect gap with $Q \neq 0$. By going beyond the first order approximation (i.e., nondipolar) and invoking two phonon processes, one can also observe two gaps simultaneously, direct and indirect, through an optical study.¹² This is the case for $\text{CeOs}_4\text{Sb}_{12}$, for which both optical and inelastic studies reveal the presence of two energy gaps.^{10,12} Currently, the physics of such spin/charge gap systems remains only partially understood, particularly the NFL behavior in the presence of a hybridization gap. In order to establish a more accurate picture and allow for theoretical developments, it is crucial to understand the nature of the hybridized bands near the Fermi level. In particular, it is extremely valuable to study systematically spin and charge gaps in various strongly correlated electron systems.

Very recently, we have observed an activation energy of about 25 meV in $\text{CeFe}_4\text{Sb}_{12}$ by Hall effect measurements.⁷ The transport pseudogap of 50 meV deduced from these experiments agrees very well with the peak observed in the optical conductivity at 50 meV in $\text{CeFe}_4\text{Sb}_{12}$,¹³ suggesting that the physics of this system is reminiscent of that found in its Os and Ru analogues, i.e., opening of a gap near E_F . In the present work, the presence of a transport gap in $\text{CeFe}_4\text{Sb}_{12}$ has been directly investigated by inelastic neutron scattering (INS) measurements. At low temperature, we observe a broad inelastic peak in the INS spectra, centered at

88 40(3) meV, as well as the absence of quasielastic scattering.
 89 The scattering intensity of the INS peak alone gives a full
 90 value of the paramagnetic effective moment of a degenerate
 91 $J=5/2$ manifold of the Ce^{3+} ions. This observation, together
 92 with the lack of quasielastic scattering, violates what is ex-
 93 pected from a crystal electric field excitation and strongly
 94 supports the existence of a spin gap near E_F , as anticipated
 95 by earlier work.^{7,13} We also show that a simple two-level
 96 phenomenological model for the spin gap allows us to ac-
 97 count quantitatively for the anomaly observed in the heat
 98 capacity, in contrast to that calculated from a crystal electric
 99 field (CEF) model. An energy gap of 36(2) meV can be ex-
 100 tracted from the heat capacity measurement, in very good
 101 agreement with the neutron work. Finally, by comparison
 102 with other Ce- and Yb-based compounds, we propose a uni-
 103 versal behavior and we show that two scaling relationships
 104 between the spin gap and the macroscopic physical proper-
 105 ties hold for a variety of systems.

106 II. EXPERIMENT

107 We have synthesized 20 g of polycrystalline samples of
 108 $\text{LaFe}_4\text{Sb}_{12}$ and $\text{CeFe}_4\text{Sb}_{12}$ by direct reaction at high tempera-
 109 ture in a carbon-coated quartz tube. The starting materials
 110 were Ce, La (99.9%), Fe (99.9999%), and Sb (99.9999%).
 111 The reacting materials were heated at 1050 °C during 48 h,
 112 water quenched, and finally annealed for 4 days at 700 °C.
 113 The samples obtained were almost single phase with minor
 114 inclusion of CeSb_2 or LaSb_2 , as indicated by x-ray diffrac-
 AQ: #15 tion and energy dispersive x-ray spectroscopy
 1 116 experiments.^{5,7,14}

117 The magnetic susceptibility has been measured between 2
 118 and 400 K in applied magnetic field of 7 T using a commer-
 119 cial MPMS superconducting quantum interference device
 120 magnetometer from Quantum Design. The heat capacity has
 121 been measured between 2 and 300 K using a microcalorim-
 122 eter and a commercial PPMS apparatus from Quantum De-
 123 sign. Inelastic neutron scattering experiments have been car-
 AQ: #24 ried out using the time-of-flight chopper spectrometer HET
 2 125 at the ISIS pulsed neutron source (UK) with incident ener-
 126 gies (E_i) of 150 and 250 meV at 5 and 300 K. The observed
 127 scattering intensity was converted into absolute units of mb/
 128 sr/meV/f.u. by normalizing the measured scattering intensity
 129 to that from a standard vanadium sample.

130 III. RESULTS AND DISCUSSION

131 A. Magnetic susceptibility

132 In Fig. 1, we report the magnetic susceptibility of
 133 $\text{CeFe}_4\text{Sb}_{12}$ between 2 and 400 K. It is to be noted that the
 134 magnetic susceptibility was measured in an applied field of
 135 7 T in order to suppress the signal of the residual free Fe
 136 impurity. This is the first determination of the magnetic sus-
 137 ceptibility of this compound above 300 K. The results below
 138 300 K are in good agreement with previous results in the
 139 literature.^{7,14–18} We note that the broad hump around
 140 125–150 K leads to an unreliable determination of both the
 141 Curie-Weiss temperature (μ_{eff}) and effective moment (θ_{CW})
 142 using data only below 300 K because the Curie-Weiss law is

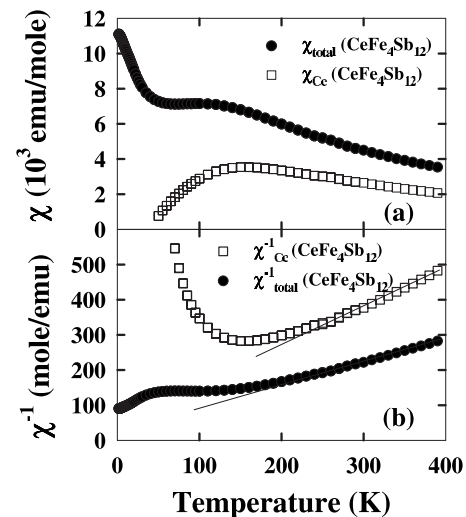


FIG. 1. (a) Magnetic susceptibility of $\text{CeFe}_4\text{Sb}_{12}$ measured at 7 T and its Ce contribution after subtraction of the iron contribution determined from the magnetic susceptibility of $\text{LaFe}_4\text{Sb}_{12}$ (see text for details). (b) Inverse of the magnetic susceptibility of $\text{CeFe}_4\text{Sb}_{12}$ measured at 7 T and its Ce contribution. The solid lines correspond to fitting of the experimental data with the Curie-Weiss equation.

not obeyed below 250 K. This can therefore explain why the
 values found in the literature for the effective paramagnetic
 moment and Curie-Weiss temperature are so different. Notably,
 the values found for μ_{eff} were between $2.4\mu_B$ and
 $4.15\mu_B$.^{7,14–18} From the present measurements, we find
 $\mu_{\text{eff}} = 3.45(1)\mu_B$ and $\theta_{\text{CW}} = -32(3)$ K for $250 < T < 400$ K.
 The value extracted here is in very good agreement with calcu-
 lations since for $\text{CeFe}_4\text{Sb}_{12}$, contributions to the magnetic sus-
 ceptibility from Ce and Fe must be taken into account. We
 therefore have used two methods for estimating the contribu-
 tion of the Ce ions to the magnetic properties to check the
 reliability of our estimation. In the first method, we use the
 following formula:

$$\mu_{\text{eff}}(\text{Ce}) = \sqrt{[\mu_{\text{eff}}(\text{exp})]^2 - [\mu_{\text{eff}}(\text{Fe})]^2}, \quad (1)$$

where $\mu_{\text{eff}}(\text{Ce})$ is the effective magnetic moment of Ce, $\mu_{\text{eff}}(\text{Fe})$
 is the effective magnetic moment of Fe and is estimated from
 the experimental value found for $\text{LaFe}_4\text{Sb}_{12}$ where only Fe
 is magnetically active, and $\mu_{\text{eff}}(\text{exp})$ is the observed total
 experimental value for $\text{CeFe}_4\text{Sb}_{12}$. Taking $\mu_{\text{eff}}(\text{Fe}) = 2.26(11)\mu_B$
 found for $\text{LaFe}_4\text{Sb}_{12}$,⁵ we find $\mu_{\text{eff}}(\text{Ce}) = 2.60(10)\mu_B$
 for the temperature range of 250–400 K. This value is in
 very good agreement with the theoretical value of $2.53\mu_B$
 for Ce^{3+} with a total angular momentum of $J=5/2$.

In the second method, we have subtracted the magnetic
 susceptibility of $\text{LaFe}_4\text{Sb}_{12}$ (Ref. 5) from that of $\text{CeFe}_4\text{Sb}_{12}$
 for the estimation of the Ce contribution $\chi(\text{Ce})$ to the mag-
 netic susceptibility in $\text{CeFe}_4\text{Sb}_{12}$. We have already used this
 procedure in a previous publication and have discussed that
 this was a reasonable procedure for $T > 50$ K.⁷ For $T > 300$
 K, we extrapolate the magnetic susceptibility of $\text{LaFe}_4\text{Sb}_{12}$
 up to 400 K using the Curie-Weiss law determined for
 $\text{LaFe}_4\text{Sb}_{12}$ above 150 K.⁵ In Fig. 1, $\chi(\text{Ce})$ and its
 inverse are reported. We see that there is a clear maximum at

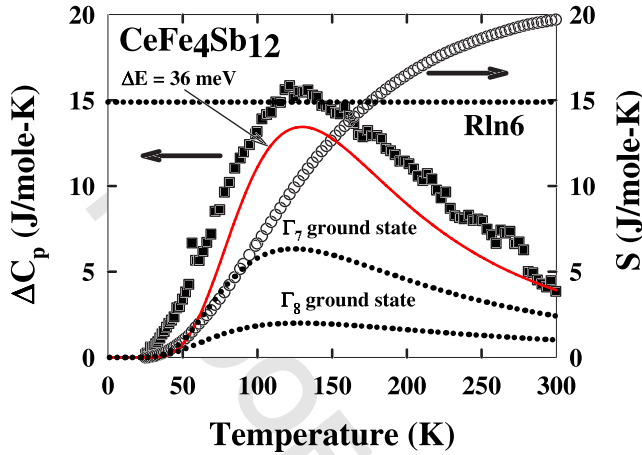


FIG. 2. (Color online) Ce contribution to the heat capacity of CeFe₄Sb₁₂ (filled symbol). The lines represent the theoretical calculations based on the pseudogap model (solid line) and on the crystal electric field models (dotted lines). Right: thermal variation of the entropy corresponding to the Ce contribution of the heat capacity of CeFe₄Sb₁₂ (open symbols).

176 about 140–150 K, in agreement with our previous results.⁷
 177 Moreover, if we fit $\chi^{-1}(\text{Ce})$ between 290 and 400 K, we find
 178 $\mu_{\text{eff}}(\text{Ce}) = 2.65(2)\mu_B$ and $\theta_{\text{CW}} = -30(7)$ K. This result is in
 179 good agreement with the one obtained from the first method.
 180 Therefore, this indicates that the contribution of the Fe to the
 181 magnetic properties is the same in CeFe₄Sb₁₂ and in
 182 LaFe₄Sb₁₂, at least at high enough T ($T > 50$ K). It is to be
 183 noted that the data of $\chi(\text{Ce})$ at low temperatures (below
 184 50 K) are not reliable due to the strong contribution of the Fe
 185 ion, as seen from the susceptibility of LaFe₄Sb₁₂,⁷ and hence
 186 not given in Fig. 1.

187 B. Heat capacity

188 Figure 2 shows the Ce contribution of the heat capacity of
 189 CeFe₄Sb₁₂, which has been obtained by subtracting the heat
 190 capacity of LaFe₄Sb₁₂ from that of CeFe₄Sb₁₂. As explained
 191 in our preliminary report,⁷ and similarly to what is observed
 192 for the magnetic susceptibility, the heat capacity of
 193 LaFe₄Sb₁₂ is larger than that of CeFe₄Sb₁₂, below 25 K. This
 194 is probably due to the larger density of states at low tempera-
 195 ture in the La compound than in the Ce compound¹⁹ and to
 196 the larger contribution of spin fluctuations related to iron in
 197 the La compound, as can be deduced from the larger Som-
 198 merfeld coefficient in LaFe₄Sb₁₂.^{5,7,20,21}

199 In Fig. 2, we observe a Schottky-type anomaly with a
 200 maximum close to 125 K. This can be explained in three
 201 ways:

202 • by considering the effect of the cubic CEF splitting on
 203 the sixfold $J=5/2$ multiplet of the Ce³⁺ ion into a doublet
 204 (Γ_7) and a quartet (Γ_8),

205 • interaction between the CEF and the Kondo effect, as
 206 we have proposed in our preliminary report,^{7,22,23} and

207 • the presence of a hybridization gap (or pseudogap), as
 208 observed in other Ce-based skutterudites.^{10,11,24}

209 First, we consider the simple case of a Schottky anomaly
 210 arising from the cubic CEF effect alone (i.e., considering a

hypothetical system where T_K is negligible with respect to
 the CEF energy gap Δ_{CEF}). Calculations (dotted lines) using
 either a doublet (Γ_7) or a quartet (Γ_8) ground state fail to
 reproduce the experimental result, particularly the magnitude
 of the peak in the specific heat measurement, as seen in Fig.
 2. This behavior is consistent with our earlier work⁷ showing
 that T_K and CEF would have the same temperature. This
 argument is reinforced by inspecting the variation of the entropy
 with temperature, found to be continuous without appearance
 of plateau at values of $R \ln 4$ or $R \ln 2$. This indicates that
 the low temperature Kondo temperature and the CEF splitting
 have the same order of magnitude.

As to the second case, there are some reports on the heat
 capacity of Kondo systems in the presence of CEF.^{22,23} How-
 ever, no simple analytical results have been reported, and the
 calculations show that the position of the heat capacity peak
 is related both to the value of the CEF splitting and to the
 Kondo temperature with a complex form. The case was con-
 sidered by Kawakami and Okiji for the cubic symmetry²²
 and by Desgranges and Rasul for a lower symmetry.²³ The
 thermal variation of the heat capacity is very close to the
 case where we can neglect the CEF [this is the case for
 which the ratio of the CEF splitting Δ_{CEF} and the high tem-
 perature Kondo temperature T_K (or T_0 symbol used in Ref.
 22) for $J=5/2$ is between 0 and 1 and tends to 0], i.e., the
 case for the fully degenerate multiplet of Ce³⁺ ion with
 $J=5/2$. However, there is no analytical expression available
 for the temperature dependence of the heat capacity in this
 case, for both the modes discussed here, so we have not
 analyzed our data based on this approach. Further, the nu-
 merical calculations show that the peak height remains al-
 most the same or reduces with the increase in the ratio of
 Δ_{CEF}/T_K , which suggests that this case is also not appropri-
 ate to explain the observed heat capacity data of CeFe₄Sb₁₂.

In the third case, where we consider that the Schottky-
 type anomaly is due to a hybridization gap (or pseudogap),
 we have the following simple phenomenological two-level
 model with a Schottky anomaly:²⁴

$$\Delta C = Nk_B \left(\frac{\Delta E}{k_B T} \right)^2 \frac{(2J+1)e^{\Delta E/k_B T}}{(2J+1 + e^{\Delta E/k_B T})^2}, \quad (2)$$

where ΔE is the hybridization gap energy. Assuming a full
 degeneracy of the ground state, $J=5/2$, we can reproduce
 well the experimental results, leading to $\Delta E = 36(2)$ meV
 (solid lines in Fig. 2). This value is to be compared with the
 value of the gap $2E_g = 50$ meV found from the Hall effect
 experiment.⁷ When considering $J=3/2$ or $1/2$, the calculated
 height of the heat capacity peak is too small, which again
 suggests that the physics of CeFe₄Sb₁₂ is governed by full
 degeneracy of the sixfold $J=5/2$ multiplet. This simple phe-
 nomenological two-level model has the advantage of its sim-
 plicity, but does not take into account the detailed structure
 of the density of states, such as the width of the upper and
 lower hybridized bands as well as a finite residual DOS in
 the gap. However, this simple model has been successfully
 used to explain the heat capacity behavior in some Kondo
 semiconductors.²⁴ Further, we note that the analysis of the
 heat capacity presented here assumes that the gap energy is

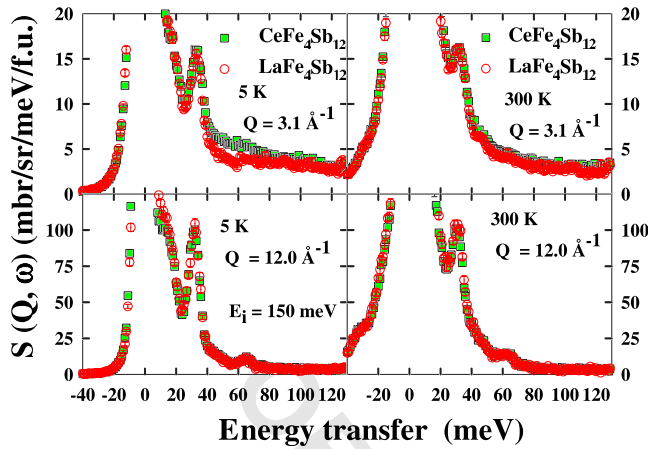


FIG. 3. (Color online) Inelastic neutron scattering spectra of $\text{CeFe}_4\text{Sb}_{12}$ and $\text{LaFe}_4\text{Sb}_{12}$ at 5 and 300 K, respectively. Data have been recorded with an incident neutron energy $E_i=150$ meV and are shown for different fixed Q values.

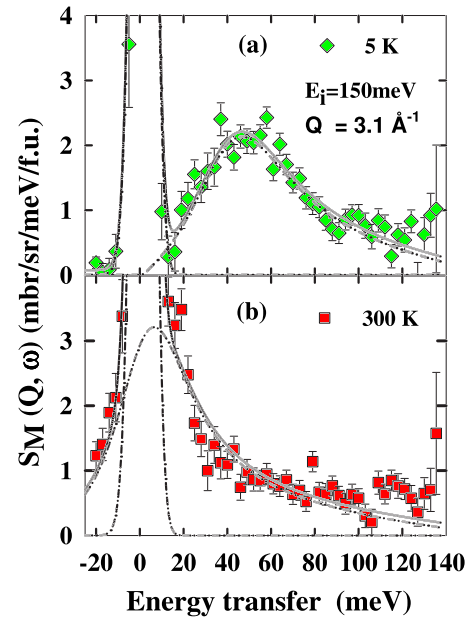


FIG. 4. (Color online) Inelastic neutron scattering spectra showing the Ce magnetic response for $\text{CeFe}_4\text{Sb}_{12}$ after subtraction of the nonmagnetic scattering at 5 and 300 K. The solid line represents the result of the refinement (see text for details). Dash-dotted lines show the separated contributions of the elastic, inelastic, and background signals.

independent of the temperature, in contrast to what is evidenced by inelastic neutron scattering experiments and discussed in the next section. At least, we cannot exclude that the formation of a hybridization gap could be influenced by its interaction with the CEF and the Kondo effect. Noticeably, in a theoretical work on the periodic Anderson model including the CEF effect, Hanzawa studied the role of the CEF effect on the formation of hybridization pseudogap²⁵ and discussed various cases depending on the relative strengths of the CEF and gap energy. When the gap and CEF energies are similar, it was found that some residual density of states exists in the pseudogap, leading to a semimetallic behavior with a large value of the Sommerfeld coefficient, as observed for CeNiSn (Ref. 26) and here in $\text{CeFe}_4\text{Sb}_{12}$.⁷

281 C. Inelastic neutron scattering

282 Figure 3 shows the inelastic neutron scattering spectra of
283 $\text{CeFe}_4\text{Sb}_{12}$ and $\text{LaFe}_4\text{Sb}_{12}$ for low $Q(3.1 \text{ \AA}^{-1})$ and high
284 $Q(12 \text{ \AA}^{-1})$; here Q is the magnitude of the wave vector trans-
285 fer ($|Q|$) at 5 and 300 K. We can see that at 5 K and at low
286 Q , between 40 and 90 meV energy transfer, the scattering
287 intensity for $\text{CeFe}_4\text{Sb}_{12}$ is higher than that for $\text{LaFe}_4\text{Sb}_{12}$.
288 This clearly indicates the presence of magnetic scattering
289 above 40 meV and at 5 K in $\text{CeFe}_4\text{Sb}_{12}$. Furthermore, the
290 scattering intensity at high Q is almost identical in both
291 $\text{CeFe}_4\text{Sb}_{12}$ and $\text{LaFe}_4\text{Sb}_{12}$. It is to be noted that the intensity
292 of magnetic scattering will decrease with increasing Q fol-
293 lowing the magnetic form factor squared, $F^2(Q)$, while the
294 intensity of phonon scattering will increase with Q as Q^2 .
295 The observed similar scattering at high Q in both $\text{CeFe}_4\text{Sb}_{12}$
296 and $\text{LaFe}_4\text{Sb}_{12}$ indicates that they have similar phonon scat-
297 tering contributions, as expected. The magnetic scattering in
298 $\text{CeFe}_4\text{Sb}_{12}$ has been extracted using a method described in
299 Ref. 9,

$$300 \quad S(Q, \omega)_{\text{mag}} = S(Q, \omega)_{\text{CeFe}_4\text{Sb}_{12}} - S(Q, \omega)_{\text{LaFe}_4\text{Sb}_{12}} \alpha,$$

301 where $\alpha=0.94$ is the ratio of the total scattering cross section
302 of $\text{LaFe}_4\text{Sb}_{12}$ and $\text{CeFe}_4\text{Sb}_{12}$. Figure 4 shows the estimated

magnetic scattering in $\text{CeFe}_4\text{Sb}_{12}$ at 5 and 300 K. Interest- 303
ingly, at 5 K, we can see a broad inelastic peak centered 304
around 50 meV, while at 300 K, the magnetic response be- 305
comes clearly of the quasielastic type. This kind of tempera- 306
ture dependence of the magnetic signal has been observed in 307
other skutterudite compounds such as $\text{CeRu}_4\text{Sb}_{12}$ (Ref. 9) 308
and $\text{CeOs}_4\text{Sb}_{12}$ (Ref. 10) and also in the Kondo semiconductor 309
 $\text{Ce}_3\text{Bi}_4\text{Pt}_3$ (Ref. 27) and the metallic Kondo compound 310
 YbAl_3 .²⁸ This observed temperature dependence of inelastic 311
response is in agreement with the theoretical calculations of 312
the dynamical susceptibility for Kondo insulators.²⁴ Further- 313
more, it is interesting to note the value of the threshold en- 314
ergy is ~ 16 meV and that of the peak position is ~ 50 meV; 315
the latter is nearly three times the former. We will discuss this 316
point in more detail later in this section. We have fitted the 317
broad magnetic inelastic peak at ~ 50 meV in the magnetic 318
response of $\text{CeFe}_4\text{Sb}_{12}$ at 5 K using a Lorentzian spectral 319
function that allows a determination of the energy of the 320
inelastic peak, referred to as spin-gap energy Δ_{spin} 321
 $=40(3)$ meV, and the linewidth [half-width at half maximum 322
(HWHM)] of about $27(3)$ meV. At 300 K, the response is 323
better fitted with a quasielastic peak (centered at zero energy) 324
with a linewidth of $20(3)$ meV. It is interesting to compare 325
the value of the susceptibility estimated through inelastic 326
neutron scattering measurements with that determined using 327
a conventional magnetometer. Using the sum rule for the 328
uniform bulk susceptibility [the so-called Kramers-Krönig 329
relation,²⁸ $\int \chi''(\omega)/\omega d\omega = \chi'(0)$], we have determined $\chi'(0)$ 330
 $=2.8(4) \times 10^{-3}$ emu/mole (see Fig. 1) at 5 and $2.7(2)$ 331
 $\times 10^{-3}$ at 300 K. These values are very close to the value of 332
 2.4×10^{-3} emu/mole estimated from the Ce bulk magnetic 333
susceptibility $\chi(300 \text{ K})$. Furthermore, a paramagnetic effec- 334

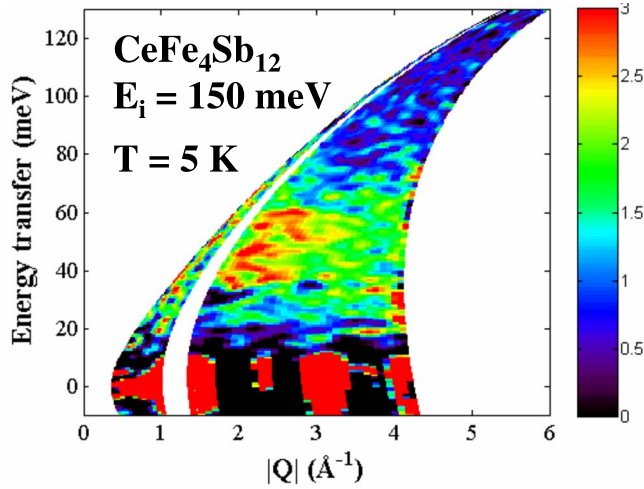


FIG. 5. (Color online) Contour map of the magnetic scattering for CeFe₄Sb₁₂ at 5 K plotted as a function of energy transfer (E) and wave vector transfer $|Q|$. The scattering intensity is color coded.

335 tive moment of $\mu_{\text{eff}}=2.3(1)\mu_B$ has been extracted using the
 336 second sum rule of $S(Q, \omega)$, $\int S(q, \omega)/F^2(Q)d\omega=48.8\mu_{\text{eff}}^2$ us-
 337 ing the 5 K data. This is in good agreement with that esti-
 338 mated from the bulk susceptibility, as discussed previously.
 339 The presence of an inelastic magnetic scattering signal
 340 near 40 meV indicates the formation of a spin gap (Δ_{spin}) in
 341 the hybridized bands near the Fermi level in CeFe₄Sb₁₂; thus,
 342 it would be interesting to see its Q dependence. The contour
 343 plot as a function of energy transfer versus $|Q|$ shown in Fig.
 344 5 for the magnetic scattering in CeFe₄Sb₁₂ at 5 K reveals a
 345 broad inelastic peak near 50 meV, whose position is nearly
 346 independent of Q . This may indicate a single ion Kondo-type
 347 response. However, the Q dependence of the energy inte-
 348 grated intensity between 40 and 65 meV for both the inci-
 349 dent energies of 150 and 250 meV exhibits a broad maxi-
 350 mum near $Q \sim 2 \text{ \AA}^{-1}$. This behavior is different from that
 351 expected for the magnetic form factor of Ce³⁺: For compari-
 352 son, we have also plotted the Ce³⁺ magnetic form factor
 353 squared [$F^2(Q)$] in Fig. 6 (solid line). At present, we do not
 354 have any clear explanation for the observed Q dependence
 355 behavior of the intensity. One of the possibilities is that it
 356 may be due to the presence of weak short range exchange

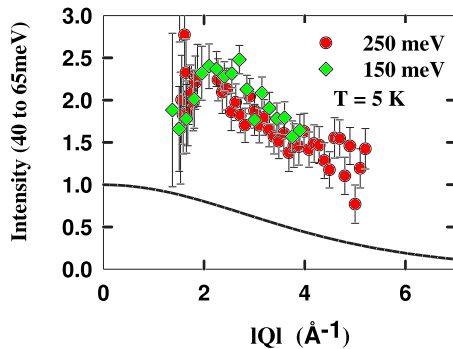


FIG. 6. (Color online) Q dependence of the energy integrated intensity between 40 and 65 meV at 5 K for an incident energy of 150 meV (green diamond) and of 250 meV (red circle).

interactions between the Ce and Fe ions, as discussed in the
 next section.

Here we will give a detailed discussion of how the thresh-
 old energy ($E_{\text{thr}}-E_f$) is related to the peak position ($E_{\text{peak}}-E_f$)
 observed in inelastic neutron scattering. Here, E_f is the posi-
 tion of the f quasiparticle peak (just above the Fermi energy
 or the middle of the gap in the DOS). In the quasiparticle
 limit (i.e., low temperature and low energy limit), the f -DOS
 should be given in terms of the (unhybridized) conduction
 band density of states, derived from the slave boson theory
 of the Anderson lattice model, assuming k -independent hy-
 bridization matrix elements,²⁴ via

$$\rho_f(E) = \left(\frac{V}{E - E_f} \right)^2 \rho_c \left[E - \left(\frac{V^2}{E - E_f} \right) \right], \quad (3)$$

where V is the renormalized hybridization matrix element.
 Further, the threshold energy is given by setting the argu-
 ment of ρ_c to its extremal values $\pm W$, where W is the width of the
 conduction band, or, in other words, the smallest value of the
 hybridization gap is caused by hybridization with conduction
 band states at either the top or the bottom of the conduction
 band. So, one has

$$\left[E - \left(\frac{V^2}{E - E_f} \right) \right] = \pm W, \quad (4)$$

which gives the band edges at

$$E = E_f + \frac{\pm W - E_f}{2} \pm \left(\sqrt{\left(\frac{\pm W - E_f}{2} \right)^2 + V^2} \right). \quad (5)$$

So, one expects the threshold energy in the f -DOS to be given by

$$(E_{\text{thr}} - E_f) = \frac{V^2}{W}. \quad (6)$$

However, the peak in the f -DOS is given by

$$\frac{\partial \rho_f}{\partial E} = 0 \quad (7)$$

or

$$(E_{\text{peak}} - E_f) = \frac{2}{\left[1 + \left(\frac{V}{E - E_f} \right)^{-2} \right]} \left(\frac{\rho_c}{\partial E} \right), \quad (8)$$

where $\rho_c \propto (E \pm W)^\alpha$ at the band edges, so $\alpha=1/2$. On solving this, one finds that the peak position is given by

$$(E_{\text{peak}} - E_f) = \frac{(2 + \alpha)}{2} \left(\frac{V^2}{W} \right). \quad (9)$$

So, with $\alpha=1/2$, we have

$$(E_{\text{peak}} - E_f) = \frac{5}{4} \left(\frac{V^2}{W} \right). \quad (10)$$

Thus, Eq. (10) shows that the peak energy ($E_{\text{peak}}-E_f$) is 5/4 times the threshold energy ($E_{\text{thr}}-E_f$)= (V^2/W) , which is smaller than what we have seen in Fig. 4 for CeFe₄Sb₁₂. This

AQ:
#7

395 could change if one introduces a k -dependent hybridization
396 or if there is a Van Hove singularity in the conduction band
397 density of states nearby.

398 Now, we discuss on the various origins of the magnetic
399 signal at 40 meV in CeFe₄Sb₁₂. There are two main possi-
400 bilities. Firstly, we are dealing with a CEF transition very
401 much broadened by the Kondo spin fluctuations. Indeed, a
402 similar inelastic signal has been observed at low tempera-
403 tures for the Kondo systems CeNi₂Ge₂ (Ref. 29) and
404 CeRu₂Si₂ (Ref. 30), where T_K is about 20 K and the CEF
405 splitting is about 300 K. However, in CeRu₂Si₂, a quasielas-
406 tic peak is also observed with a HWHM of about 1 meV.³¹
407 Thus, the case of these compounds is different from the
408 present case for which we have not observed any quasielastic
409 peak in the high-resolution INS experiment on the time-of-
410 flight spectrometer IN4.³² To further confirm the absence of
411 any magnetic scattering at low energy, we have also carried
412 out high-resolution INS measurements on CeFe₄Sb₁₂ and

AQ: #13
4 LaFe₄Sb₁₂ on the MARI spectrometer at ISIS with E_f
414 = 20 meV at 15 K. We found a similar scattering in both the
415 compounds for Q values between 0.75 and 5 Å⁻¹ (data not
416 shown here). This again supports the absence of the quasi-
417 elastic scattering in the spin gap of CeFe₄Sb₁₄. This observa-
418 tion is in agreement with our estimation of $\mu_{\text{eff}} \sim 2.3(1)\mu_B$,
419 which is close to the full theoretical value of $2.54\mu_B$, from
420 the integrated intensity of the 50 meV peak. This suggests
421 that most of the integrated intensity expected from the sum
422 rules is tied up in the high energy response, and hence there
423 is little intensity left to assign at low energy and low Q .
424 Thus, our second explanation for the magnetic signal ob-
425 served in CeFe₄Sb₁₂, and its temperature dependence, is the
426 observation of a spin gap, as mentioned previously, similar to
427 that observed in skutterudite compounds CeRu₄Sb₁₂ (Ref. 9)
428 and CeOs₄Sb₁₂,¹⁰ in the Kondo semiconductor Ce₃Bi₄Pt₃,²⁷
429 and in intermediate valence systems (IVSs) such as YbAl₃.²⁸

430 It is interesting to compare the absolute value of the spin-
431 gap energy obtained from the various different techniques in
432 CeFe₄Sb₁₂ and also to compare the spin-gap value with other
433 compounds. The value found for the spin gap from the heat
434 capacity (36 meV) agrees very well with the value extracted
435 [40(3) meV] from the Lorentzian spectral fit to the INS data.
436 This good agreement is thus a further support of our simple
437 model for the heat capacity. Furthermore, it is very interest-
438 ing to note that the value of the charge gap $\Delta_{\text{char}} \sim 50$ meV
439 observed in the optical experiment in CeFe₄Sb₁₂ (Ref. 13) is
440 similar to the spin-gap energy of $\Delta_{\text{spin}} \sim 40\text{--}50$ meV found
441 here for the inelastic neutron scattering and Hall effect
442 experiments.⁷ Thus, here the ratio between the charge gap
443 and the spin gap is about $\sim 0.8\text{--}1$. A very similar ratio of the
444 charge gap to spin gap has also been observed in the case of
445 another skutterudite compound, CeOs₄Sb₁₂.¹⁰ The absolute
446 value of the spin gap observed in CeFe₄Sb₁₂ is larger than
447 the spin-gap value of 30 and 27 meV observed in CeRu₄Sb₁₂
448 and CeOs₄Sb₁₂, respectively, which indicates the presence of
449 stronger hybridization in the former compound.

450 Now, we want to check the general validity of this phe-
451 nomenological model for IVS and Kondo semiconductors.
452 Because there are some compounds with different values of J
453 (1/2, 5/2, or 7/2), we have plotted the position of the in-
454 elastic neutron scattering peak E_{INS} in meV (see Refs. 27, 28,

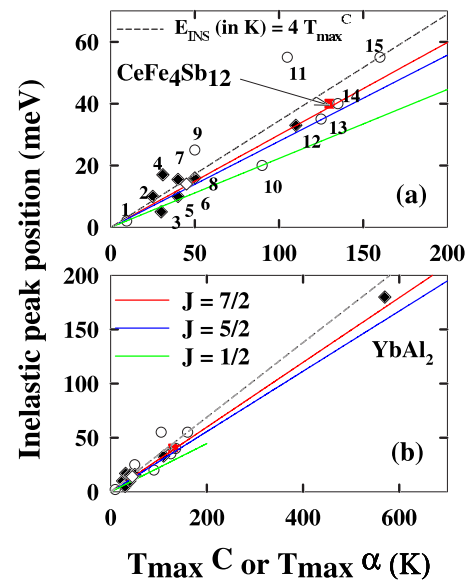


FIG. 7. (Color online) [(a) and (b)] Maximum of the INS peak E_{INS} (see Refs. 23, 24, and 36–49) vs maximum of the heat capacity T_{max}^C and of the thermal expansion T_{max}^α (see Refs. 27, 35, 39, and 49–62) in the intermediate valence systems, Kondo semiconductors. 1: CeNiSn, 2: YbCuAl, 3: YbPd₂Si₂, 4: YbCu₂Si₂, 5: YbCu₄Ag, 6: SmB₆, 7: YbB₁₂, 8: Yb_{0.75}Lu_{0.25}B₁₂, 9: Ce₃Bi₄Pt₃, 10: CePt₂Si₂, 11: CeNi, 12: YbAl₃, 13: CeRhSb, 14: CeSn₃, and 15: CePd₃. The dashed line represents the equation $E_{\text{INS}} (\text{in K}) = 4 T_{\text{max}}^C$, while the solid lines show the calculations corresponding to the ratio between ΔE and T_{max}^C in a simple two-level phenomenological model for various J values (see text for details). The symbols used in (b) have same meaning as in (a).

and 34–47) versus the temperature of the maximum to the
Ce contribution of the heat capacity T_{max}^C or thermal expan-
sion, if the heat capacity data are not available, for the dif-
ferent compounds found in the literature (see Refs. 33, 34,
46, and 48–61). This is shown in Fig. 7, where we can see that
the majority of the compounds are around a straight line for
which we have E_{INS} (in kelvin) equal to about four times
 T_{max}^C . In a solid line, we have also plotted the case where Eq.
(2) is applied for different values of the kinetic moment J . It
is interesting to note that the calculations of Hanzawa²⁵ of
the specific heat for the different kinetic moments $J = 5/2$ and
7/2 lead to almost the same ratio (about 3.5) between the
value of the spin gap ΔE (equal here to E_{INS}) and the tem-
perature of the maximum of the heat capacity in using the
periodic Anderson model rather than our phenomenological
two-level model. This provides further support for using the
simple phenomenological model in our heat capacity data
analysis. However, we note that there are some disagree-
ments for CeNi, Ce₃Bi₄Pt₃, and CePt₂Si₂. For CeFe₄Sb₁₂, we
have used the value of E_{INS} from the fit in Fig. 4 that gave a
good agreement between the heat capacity and INS experi-
ments. Obviously, the deviations observed from the straight
line should be due to the too great simplicity of our phenom-
enological model because it ignores the details of the DOS
around the hybridization gap. Clearly, it would be very inter-
esting to make the heat capacity and/or thermal expansion
measurements up to 300 K on CeRu₄Sb₁₂ and CeOs₄Sb₁₂ to

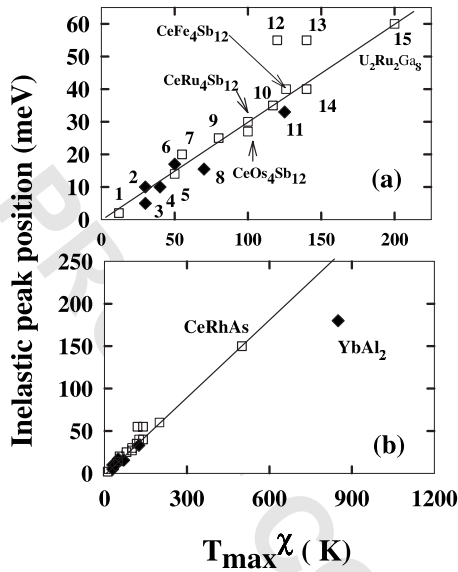


FIG. 8. [(a) and (b)] Maximum of the INS peak E_{INS} (see Refs. 27, 28, 34–46, 65, and 66) vs maximum of the magnetic susceptibility T_{max}^{χ} (see Refs. 27, 28, 34–47, 65, and 66) in the intermediate valence systems, Kondo semiconductors. 1: CeNiSn, 2: YbCuAl, 3: YbPd₂Si₂, 4: YbCu₂Si₂, 5: SmB₆, 6: YbCu₄Ag, 7: CePt₂Si₂, 8: YbB₁₂, 9: Ce₃Bi₄Pt₃, 10: CeRhSb, 11: YbAl₃, 12: CePd₃, 13: CeNi, 14: CeSn₃, and 15: U₂RuGa₈. The solid line is a guide to the eyes. The symbols used in (b) have the same meaning as in (a).

test whether our simple phenomenological model also works in this case.

According to the single impurity model,⁶² we can estimate the high temperature Kondo temperature T_K through the maximum $T_{\text{max}}(\chi)$ in the bulk susceptibility as $T_K = 3T_{\text{max}}(\chi)$. Therefore, it would be interesting to show a universal relation between the inelastic peak position (or spin-gap energy) and the high temperature Kondo temperature T_K or $T_{\text{max}}(\chi)$, as shown in Ref. 10. In Fig. 8, we have plotted the peak position of the inelastic neutron scattering versus $T_{\text{max}}(\chi)$ for many Ce- and Yb-based intermediate valence compounds. We can see that the excellent universal scaling relation is observed between $T_{\text{max}}(\chi)$ or T_K (Refs. 24, 28, 33, 36, 39, 50, 51, 55, 60, and 63–66) and the inelastic peak position corresponding to the spin gap (see Refs. 27, 28, 34–47, and 63–66) in all these compounds, notably for the case of three different $\text{CeM}_4\text{Sb}_{12}$ ($M=\text{Fe, Ru, and Os}$) skutterudite compounds.

546
547
548

*Author to whom correspondence should be addressed; d.t.adroja@r-lac.uk

†Present address: Institute of Solid State Physics, TU Vienna, Wiedner Hauptstr. 8-10, 1040 Vienna, Austria.

¹B. C. Sales, D. Mandrus, B. C. Chakoumakos, V. Keppens, and J. R. Thompson, Phys. Rev. B **56**, 15081 (1997); V. Keppens, D.

IV. CONCLUSIONS

500

We have carried out magnetic susceptibility, heat capacity, and inelastic neutron scattering measurements on $\text{CeFe}_4\text{Sb}_{12}$ in order to understand the nature of $4f$ electrons in this compound and especially to find out whether there exists a spin gap or not. Our inelastic neutron scattering study clearly reveals the presence of spin gap $\Delta_{\text{spin}} \sim 40(3)$ meV in $\text{CeFe}_4\text{Sb}_{12}$, which is also supported through our heat capacity measurements as well as published Hall effect measurements.⁷ Further, we found that the spin-gap energy is independent of Q , which indicates that single-ion-type interactions play an important role in the spin-gap formation. On the other hand, the energy integrated magnetic intensity between 40 and 65 meV shows a broad maximum at $Q \sim 2 \text{ \AA}^{-1}$, which might suggest the presence of some weak intersite correlations. The fact that Ce-Ce distances are larger (7.91 Å) in $\text{CeFe}_4\text{Sb}_{12}$ and that the maximum in the susceptibility of $\text{Ce}_{1-x}\text{La}_x\text{Ru}_4\text{Sb}_{12}$ is independent of La concentration⁷ furthermore supports the single impurity-type behavior of the Ce ions. Thus, it is likely possible that weak intersite correlations may exist between the Ce and Fe atoms, due to the shorter Ce-Fe distance (3.95 Å) as well as the paramagnetic nature of the Fe ion in $\text{CeFe}_4\text{Sb}_{12}$, which are most likely responsible for the observed Q -dependence intensity. We have also found a universal scaling relation between the spin-gap energy and the temperature, at which the bulk susceptibility and also the heat capacity (or thermal expansion) exhibit a maximum for many Ce and Yb compounds. We have presented theoretical calculations showing a relation between the threshold energy and the peak position observed in the inelastic response of spin-gap systems.

An important role of the Fe ion in $\text{CeFe}_4\text{Sb}_{12}$ can be seen when we compare the value of spin-gap energy of 40–50 meV, which are larger than 30 meV in $\text{CeRu}_4\text{Sb}_{12}$ and 27 meV in $\text{CeOs}_4\text{Sb}_{12}$. This is also true for the Pr-based skutterudite superconductors: $\text{PrT}_4\text{Sb}_{12}$ ($T=\text{Fe, Ru, and Os}$) all having a singlet ground state.^{67–69} The Pr compounds with $T=\text{Os}$ and Ru are superconducting with $T_c \sim 1.9$ and 1 K, respectively, but no superconductivity has been observed in the $T=\text{Fe}$ compound. This observation again suggests the special role played by the Fe ion in both the Ce- and Pr-based skutterudite compounds.

ACKNOWLEDGMENTS

542

We acknowledge interesting discussions on the neutron scattering results with E. A. Goremychkin, B. D. Rainford, and K. A. McEwen.

Mandrus, B. C. Sales, B. C. Chakoumakos, P. Dai, R. Caillat, and A. Borchshevski, Nature (London) **395**, 876 (1998).

²E. D. Bauer, N. A. Frederick, P.-C. Ho, V. S. Zapf, and M. B. Maple, Phys. Rev. B **65**, 100506(R) (2002).

³H. Sugawara, T. D. Matsuda, K. Abe, Y. Aoki, H. Sato, S. Nojiri, Y. Inada, R. Settai, and Y. Onuki, Phys. Rev. B **66**, 134411

- 561 (2002).
562 ⁴C. Sekine, T. Uchiumi, I. Shirovani, and T. Yagi, Phys. Rev. Lett.
563 **79**, 3218 (1997).
564 ⁵R. Viennois, S. Charar, D. Ravot, P. Haen, A. Mauger, S. Pas-
565 chen, A. Bientien, and F. Steglich, Eur. Phys. J. B **46**, 257
566 (2005).
567 ⁶N. Takeda and M. Ishikawa, J. Phys. Soc. Jpn. **69**, 868 (2000).
568 ⁷R. Viennois, D. Ravot, F. Terki, C. Hernandez, S. Charar, P. Haen,
569 S. Paschen, and F. Steglich, J. Magn. Magn. Mater. **272-276**,
570 e113 (2004); R. Viennois, S. Charar, D. Ravot, A. Mauger, P.
571 Haen, and J. C. Tedenac, J. Phys.: Condens. Matter **18**, 5371
572 (2006).
573 ⁸S. V. Dordevic, N. R. Dilley, E. D. Bauer, D. N. Basov, M. B.
574 Maple, and L. Degiorgi, Phys. Rev. B **60**, 11321 (1999).
575 ⁹D. T. Adroja, J.-G. Park, K. A. McEwen, N. Takeda, M. Ishikawa,
576 and J.-Y. So, Phys. Rev. B **68**, 094425 (2003).
577 ¹⁰D. T. Adroja, J.-G. Park, E. A. Goremychkin, K. A. McEwen, N.
578 Takeda, B. D. Rainford, K. S. Knight, J. W. Taylor, J. Park, H.
579 C. Walker, R. Osborn, and P. S. Riseborough, Phys. Rev. B **75**,
580 014418 (2007).
581 ¹¹M. J. Rozenberg, G. Kotliar, and H. Kajueter, Phys. Rev. B **54**,
582 8452 (1996).
583 ¹²M. Matsunami, H. Okumura, T. Namba, H. Sugawar, and H. Sato,
584 J. Phys. Soc. Jpn. **72**, 2722 (2003).
585 ¹³M. Matsunami, H. Okamura, T. Nanba, H. Sugawara, and H.
586 Sato, J. Magn. Magn. Mater. **272-276**, e41 (2004).
587 ¹⁴L. Chapon, D. Ravot, and J.-C. Tedenac, J. Alloys Compd. **282**,
588 58 (1999).
589 ¹⁵M. E. Danebrock, C. B. H. Evers, and W. Jeischko, J. Phys.
590 Chem. Solids **57**, 381 (1996).
591 ¹⁶G. P. Meisner and D. T. Morelli, J. Appl. Phys. **77**, 3777 (1995).
592 ¹⁷D. A. Gajewski, N. R. Dilley, E. D. Bauer, E. J. Freeman, R.
593 Chau, M. B. Maple, D. Mandrus, B. C. Sales, and A. Lacerda, J.
594 Phys.: Condens. Matter **10**, 6973 (1998).
595 ¹⁸B. Chen, J.-H. Xu, C. Uher, D. T. Morelli, G. P. Meisner, J. P.
596 Fleurial, T. Caillat, and A. Borshchevsky, Phys. Rev. B **55**, 1476
597 (1997).
598 ¹⁹K. Nouneh, A. H. Rashek, S. Auluck, I. V. Kityk, R. Viennois, S.
599 Benet, and S. Charar, J. Alloys Compd. **437**, 39 (2007).
600 ²⁰R. Viennois, F. Terki, A. Errebah, S. Charar, M. Averous, D.
601 Ravot, J. C. Tedenac, P. Haen, and C. Sekine, Acta Phys. Pol. B
602 **34**, 1221 (2003).
603 ²¹K. Nouneh, R. Viennois, I. V. Kityk, F. Terki, S. Charar, S. Benet,
604 and S. Paschen, Phys. Status Solidi B **241**, 3069 (2004).
605 ²²N. Kawakami and A. Okiji, J. Magn. Magn. Mater. **52**, 220
606 (1985).
607 ²³H. U. Desgranges and J. W. Rasul, Phys. Rev. B **36**, 328 (1987).
608 ²⁴P. S. Riseborough, Adv. Phys. **49**, 257 (2000); Phys. Rev. B **45**,
609 13984 (1992); P. Coleman, arXiv:cond-mat/0612006 (unpub-
610 lished).
611 ²⁵K. Hanzawa, J. Phys. Soc. Jpn. **71**, 1481 (2002).
612 ²⁶K. Izawa, T. Suzuki, T. Fujita, T. Takabatake, G. Nakamoto, H.
613 Fujii, and K. Maezawa, Phys. Rev. B **59**, 002599 (1999).
614 ²⁷A. Severing, J. D. Thompson, P. C. Canfield, Z. Fisk, and P. S.
615 Riseborough, Phys. Rev. B **44**, 6832 (1991).
616 ²⁸A. P. Murani, Phys. Rev. B **50**, 9882 (1994).
617 ²⁹C. D. Frost, B. D. Rainford, F. V. Carter, and S. S. Saxena,
618 Physica B **276**, 290 (2000).
619 ³⁰D. T. Adroja and B. D. Rainford (unpublished).
620 ³¹A. Severing, E. Holland-Moritz, and B. Frick, Phys. Rev. B **39**,
4164 (1989).
621 ³²R. Viennois, L. Girard, D. Ravot, H. Mutka, M. Koza, F. Terki, S.
622 Charar, and J. C. Tedenac, Physica B **350**, e403 (2004).
623 ³³C. Ayache, J. Beille, E. Bonjour, R. Calemczuk, G. Creuzet, D.
624 Gignoux, A. Najib, D. Schmitt, J. Viron, and M. Zerguine, J.
625 Magn. Magn. Mater. **63-64**, 329 (1987).
626 ³⁴D. Gignoux, D. Schmitt, M. Zerguine, and A. P. Muarani, J.
627 Magn. Magn. Mater. **76-77**, 401 (1988).
628 ³⁵A. P. Murani, Phys. Rev. B **28**, 2308 (1983).
629 ³⁶R. M. Galera, A. P. Murani, J. Pierre, and K. R. A. Ziebeck, J.
630 Magn. Magn. Mater. **63-64**, 594 (1987).
631 ³⁷T. J. Sato, H. Kadowaki, H. Yoshizawa, T. Ekino, T. Takabatake,
632 H. Fujii, L. P. Regnault, and Y. Isikawa, J. Phys.: Condens.
633 Matter **7**, 8009 (1995).
634 ³⁸A. D. Christianson, V. R. Fanelli, J. M. Lawrence, E. A. Goremy-
635 chkin, R. Osborn, E. D. Bauer, J. L. Sarrao, J. D. Thompson, C.
636 D. Frost, and J. L. Zarestky, Phys. Rev. Lett. **96**, 117206 (2006).
637 ³⁹A. Severing, A. P. Murani, J. D. Thompson, Z. Fisk, and C.-K.
638 Loong, Phys. Rev. B **41**, 1739 (1990).
639 ⁴⁰A. P. Murani, W. C. M. Mattens, F. R. de Boer, and G. H. Lander,
640 Phys. Rev. B **31**, 52 (1985).
641 ⁴¹L. Menon, D. T. Adroja, B. D. Rainford, S. K. Malik, and W. B.
642 Yelon, Solid State Commun. **112**, 85 (1999).
643 ⁴²J. M. Mignot, P. A. Alekseev, K. S. Nemkovski, L.-P. Regnault, F.
644 Iga, and T. Takabatake, Phys. Rev. Lett. **94**, 247204 (2005).
645 ⁴³J. M. Mignot and P. A. Alekseev, Physica B **215**, 99 (1995).
646 ⁴⁴U. Walter, E. Holland-Moritz, and U. Steigenberger, Z. Phys. B:
647 Condens. Matter **89**, 169 (1992).
648 ⁴⁵E. S. Clementyev, J. M. Mignot, P. A. Alekseev, V. N. Lazukov,
649 E. V. Nefedova, I. P. Sadikov, M. Braden, R. Kahn, and G.
650 Lapertot, Phys. Rev. B **61**, 6189 (2000).
651 ⁴⁶W. Weber, E. Holland-Moritz, and A. P. Murani, Z. Phys. B:
652 Condens. Matter **76**, 229 (1989).
653 ⁴⁷A. P. Murani, A. D. Taylor, R. Osborn, and Z. A. Bowden, Philos.
654 Mag. B **65**, 1333 (1992).
655 ⁴⁸G. H. Kwei, J. M. Lawrence, P. C. Canfield, W. P. Beyermann, J.
656 D. Thompson, Z. Fisk, A. C. Lawson, and J. A. Goldstone, Phys.
657 Rev. B **46**, 8067 (1992).
658 ⁴⁹R. Takke, M. Nicksch, W. Assmus, B. Lüthi, R. Pott, R. Schefzyk,
659 and D. K. Wohlleben, Z. Phys. B: Condens. Matter **44**, 33
660 (1981).
661 ⁵⁰J. G. Sereni, in *Handbook on Chemistry and Physics of Rare-*
662 *Earth*, edited by K. A. Gschneider, Jr. and L. Eyring (■, ■,
663 #10 1991), p. 1.
664 ⁵¹Y. Uwatoko, G. Ooomi, T. Takabatake, and H. Fujii, J. Magn.
665 Magn. Mater. **104-107**, 643 (1992).
666 ⁵²S. Nishigori, Hiroshi Goshima, Takashi Suzuki, Toshizo Fujita,
667 Go Nakamoto, Hiroaki Tanaka, Toshiro Takabatake, and Hi-
668 ronobu Fujii, J. Phys. Soc. Jpn. **65**, 2614 (1996).
669 ⁵³A. L. Cornelius, J. M. Lawrence, T. Ebihara, P. S. Riseborough,
670 C. H. Booth, M. F. Hundley, P. G. Pagliuso, J. L. Sarrao, J. D.
671 Thompson, M. H. Jung, A. H. Lacerda, and G. H. Kwei, Phys.
672 Rev. Lett. **88**, 117201 (2002).
673 ⁵⁴M. J. Besnus, P. Haen, N. Hamdaoui, A. Herr, and A. Meyer,
674 Physica B **163**, 571 (1990).
675 ⁵⁵R. Pott, R. Schefzyk, D. Wohlleben, and A. Junod, Z. Phys. B:
676 Condens. Matter **44**, 17 (1981).
677 ⁵⁶F. Iga, M. Kasaya, and T. Kasuya, J. Magn. Magn. Mater. **76-77**,
678 156 (1988).
679 ⁵⁷D. Mandrus, J. L. Sarrao, A. Lacerda, A. Migliori, J. D. Thomp-
680

- 681 son, and Z. Fisk, Phys. Rev. B **49**, 16809 (1994).
 682 ⁵⁸Y. Uwatoko, G. Oomi, J. D. Thompson, P. C. Canfield, and Z.
 683 Fisk, Physica B **186-188**, 593 (1993).
 684 ⁵⁹M. J. Besnus, M. Benakki, A. Braghta, H. Danan, G. Fischer, J. P.
 685 Kappler, A. Meyer, and P. Panissod, J. Magn. Magn. Mater.
 686 **76-77**, 471 (1988).
 687 ⁶⁰R. Hauser, T. Ishii, Y. Uwatoko, G. Oomi, E. Bauer, and E. Gratz,
 688 J. Magn. Magn. Mater. **157**, 679 (1996).
 689 ⁶¹A. Iandelli and A. Palenzona, J. Chem. Soc. Dalton Trans. **29**,
 690 293 (1972); B. Appa Rao, P. Kistaiah, and K. Satyanarayana
 691 Murthy, Mater. Lett. **9**, 410 (1990); F. Merlo, Thermochem. Acta
 692 **64**, 115 (1983).
 693 ⁶²N. E. Bickers, D. L. Cox, and J. W. Wilkins, Phys. Rev. Lett. **54**,
 694 230 (1985).
 695 ⁶³M. J. Besnus, M. Benakki, A. Braghta, H. Danan, G. Fischer, J. P.
 696 Kappler, A. Meyer, and P. Panissod, J. Magn. Magn. Mater.
 697 **76-77**, 471 (1988).
 64 J. M. Lawrence, P. S. Riseborough, and R. D. Parks, Rep. Prog.
 Phys. **44**, 1 (1981). **698**
 65 D. T. Adroja, J.-G. Park, K. A. McEwen, K. Shigetoh, T.
 Sasakawa, T. Takabatake, and J.-Y. So, Physica B **378**, 788 **699**
 (2006). **700**
 66 R. Troć, D. T. Adroja, and R. I. Bewley, ISIS Experimental Re- **701**
 port No. ■, 2005 (unpublished). **702** **AQ**
 67 E. A. Goremychkin, R. Osborn, E. D. Bauer, M. B. Maple, N. A. **703**
 Frederick, W. M. Yuhasz, F. M. Woodward, and J. W. Lynn, **704** **#11**
 Phys. Rev. Lett. **93**, 157003 (2004). **705**
 68 D. T. Adroja, J.-G. Park, E. A. Goremychkin, N. Takeda, M. Ish- **706**
 ikawa, K. A. McEwen, R. Osborn, A. D. Hillier, and B. D. **707**
 Rainford, Physica B **359**, 983 (2005); D. T. Adroja *et al.* (un- **708** **AQ**
 published) **709** **#12**
 69 E. Bauer, A. Grytsiv, P. Rogl, W. Kockelmann, A. D. Hillier, E. **710**
 A. Goremychkin, D. T. Adroja, and J.-G. Park, J. Magn. Magn. **711**
 Mater. **310**, 286 (2007). **712**
713
714

AUTHOR QUERIES —

- #1 pls. check definition of EDX.
- #2 pls. spell out MPMS, PPMS, HET.
- #3 pls. check insertion of "was."
- #4 pls. spell out MARI.
- #5 pls. check change from "45" to "46"
- #6 pls. check insertion of "rather."
- #7 Pls. be aware that although a caption makes reference to color online, figures in print will appear in black and white.
- #8 Pls. update Ref. 24 (last entry).
- #9 Pls. update Ref. 30.
- #10 Pls. supply publisher name and city in Ref. 50.
- #11 Pls. update Ref. 66.
- #12 Au-Pls. update Ref. 68, last entry; list all authors.